

ARTICLE

Open Access

Recombinant milk fat globule-EGF factor-8 reduces apoptosis via integrin β 3/FAK/PI3K/AKT signaling pathway in rats after traumatic brain injury

Yong-Yue Gao¹, Zi-Huan Zhang², Zong Zhuang¹, Yue Lu¹, Ling-Yun Wu¹, Zhen-nan Ye³, Xiang-Sheng Zhang¹, Chun-Lei Chen⁴, Wei Li¹ and Chun-Hua Hang¹

Abstract

Accumulating evidence suggests neuronal apoptosis has the potential to lead to more harmful effects in the pathological processes following traumatic brain injury (TBI). Previous studies have established that milk fat globule-EGF factor-8 (MFG-E8) provides neuroprotection through modulation of inflammation, oxidative stress, and especially apoptosis in cerebral ischemia and neurodegenerative disease. However, the effects of MFG-E8 on neuronal apoptosis in TBI have not yet been investigated. Therefore, we explored the role of MFG-E8 on anti-apoptosis and its potential mechanism following TBI. In the first set of experiments, adult male Sprague–Dawley (SD) rats were randomly divided into Sham and TBI groups that were each further divided into five groups representing different time points (6 h, 24 h, 72 h, and 7 days) ($n = 9$ each). Western blotting, quantitative real-time PCR, and immunofluorescence staining were performed to identify the expression and cellular localization of MFG-E8. In the second set of experiments, four groups were randomly assigned: Sham group, TBI + Vehicle group, and TBI + rhMFG-E8 (1 and 3 μ g) ($n = 15$). Recombinant human MFG-E8 (rhMFG-E8) was administrated as two concentrations through intracerebroventricular (i.c.v.) injection at 1 h after TBI induction. Brain water content, neurological severity score, western blotting, and immunofluorescence staining were measured at 24 and 72 h following TBI. In the final set of experiments, MFG-E8 siRNA (500 pmol/3 μ l), integrin β 3 siRNA (500 pmol/3 μ l), and PI3K inhibitor LY294002 (5 and 20 μ M) were injected i.c.v. and thereafter rats exposed to TBI. Western blotting, immunofluorescence staining, brain water content, neurological severity score, and Fluoro-Jade C (FJC) staining were used to investigate the effect of the integrin- β 3/FAK/PI3K/AKT signaling pathway on MFG-E8-mediated anti-apoptosis after TBI. The expression of MFG-E8 was mainly located in microglial cells and increased to peak at 24 h after TBI. Treatment with rhMFG-E8 (3 μ g) markedly decreased brain water content, improved neurological deficits, and reduced neuronal apoptosis at 24 and 72 h after TBI. rhMFG-E8 significantly enhanced the expression of integrin- β 3/FAK/PI3K/AKT pathway-related components. Administration of integrin- β 3 siRNA and LY294002 (5 and 20 μ M) abolished the effect of rhMFG-E8 on anti-apoptosis and neuroprotection after TBI. This study demonstrated for the first time that rhMFG-E8 inhibits neuronal apoptosis and offers neuroprotection. This is suggested to occur through the modulation of the integrin- β 3/FAK/PI3K/AKT signaling pathway, highlighting rhMFG-E8 as a potentially promising therapeutic strategy for TBI patients.

Correspondence: Wei Li (lwzlw@126.com) or C.-H. Hang (hang_neurosurgery@163.com)

¹Department of Neurosurgery, The Affiliated Drum Tower Hospital, School of Medicine, Nanjing University, Zhongshan Road 321, Nanjing 210008 Jiangsu Province, PR China

²Department of Neurosurgery, The First Affiliated Hospital of Wannan Medical College, Wuhu, Anhui Province, PR China

Full list of author information is available at the end of the article.

Edited by A. Verkhratsky

Introduction

Traumatic brain injury (TBI) remains a significant health care issue around the world¹. Although the primary insult at the moment of impact remains the major outcome determining factor, secondary brain injury caused

© The Author(s) 2018



Open Access This article is licensed under a Creative Commons Attribution 4.0 International License, which permits use, sharing, adaptation, distribution and reproduction in any medium or format, as long as you give appropriate credit to the original author(s) and the source, provide a link to the Creative Commons license, and indicate if changes were made. The images or other third party material in this article are included in the article's Creative Commons license, unless indicated otherwise in a credit line to the material. If material is not included in the article's Creative Commons license and your intended use is not permitted by statutory regulation or exceeds the permitted use, you will need to obtain permission directly from the copyright holder. To view a copy of this license, visit <http://creativecommons.org/licenses/by/4.0/>.

by subsequent pathological processes may persist for a longer period and aggravate TBI damage². Despite recent developments in understanding the pathological processes of TBI, effective therapeutic strategies are yet to emerge. Searching for an effective treatment that improves the outcome of TBI patients is therefore urgently needed.

Milk fat globule-epidermal growth factor [EGF]-factor 8 (MFG-E8), also known as lactadherin in humans, is a secreted multifunctional glycoprotein originally discovered in mouse milk and the mammary epithelium³. Further studies identified MFG-E8 as an intrinsic component of the milk fat globule membrane⁴. MFG-E8 has aroused widespread interest over the last few years, being ascribed a mediator role in cell–cell interactions involved in various biological processes and pathophysiological functions, including the innate immune response⁵, angiogenesis⁶, and fertilization⁷. To this end, several cell types can express MFG-E8, including mammary epithelial cells, macrophages, oligodendrocytes, endothelial cells, as well as intestinal and retinal epithelial cells⁸.

In the central nervous system, MFG-E8 is mainly expressed in microglia, while small amounts of MFG-E8 could also be seen in astrocytes and neurons^{9,10}. In previous studies, pharmacological upregulation of MFG-E8 expression was shown to have neuroprotective effects in Alzheimer's disease (AD)¹¹. Furthermore, the administration of recombinant human MFG-E8 (rhMFG-E8) could attenuate cerebral injury through suppression of inflammation and apoptosis in cerebral ischemia^{5,12}. Both in vitro and in vivo, MFG-E8 promotes the engulfment of apoptosis cells by acting as a conjunctive molecule that combines with phosphatidylserine and $\alpha_v\beta_3$ -integrin on apoptotic cells and macrophages, respectively^{13–15}. Meanwhile, focal adhesion kinase (FAK), as the downstream molecule of the integrin receptor, activates the downstream effector protein kinase B (AKT) to inhibit apoptosis^{16,17}. Additionally, rhMFG-E8 exerts beneficial effects in the models of AD and subarachnoid hemorrhage by reducing oxidative stress through modulation of the integrin receptor and heme oxygenase-1 (HO-1)^{11,18}.

To date, the effects of MFG-E8 in TBI have not been investigated. It is hypothesized that MFG-E8 may have a favorable influence during the pathological process of TBI. Therefore, the aim of the present study was to investigate the efficacy of MFG-E8 in a TBI mouse model.

Materials and methods

Animals preparation

Adult male Sprague–Dawley (SD) rats weighing 250–300 g were purchased from the Experimental Animal Center of Drum Tower Hospital and housed in a 12 h light/dark cycle room. All rats were allowed free

access to food and water under conditions of controlled humidity and temperature ($24 \pm 0.5^\circ\text{C}$). The experimental protocols and procedures were approved by the Institutional Animal Care and Use Committee at Drum Tower Hospital and conformed to the National Institutes of Health (NIH) Guide for the Care and Use of Laboratory Animals.

Rat TBI model

Experimental TBI models used in this study were performed as described in previous studies^{19,20}. Briefly, rats were placed in a stereotaxic frame after intraperitoneal anesthesia with sodium pentobarbital (50 mg/kg). After disinfection, a 2.0 cm midline scalp incision was made and the skull was exposed. On the left parietal cortex, a 6-mm craniotomy was performed through the skull; the center of the hole was 2.5 mm lateral to the midline on the mid-coronal plane. The dura was left intact during the operation. The impact was performed by releasing a 40 g weight onto the dura from a height of 25 cm along a steel shaft, which translated to $1000 \times \text{g/cm}$. By this time, the scalp wound was thoroughly disinfected and closed with suture. Sham animals were subjected to the same procedures without injury. Then rats were returned to the cages and maintained at a temperature of $24.0 \pm 0.5^\circ\text{C}$.

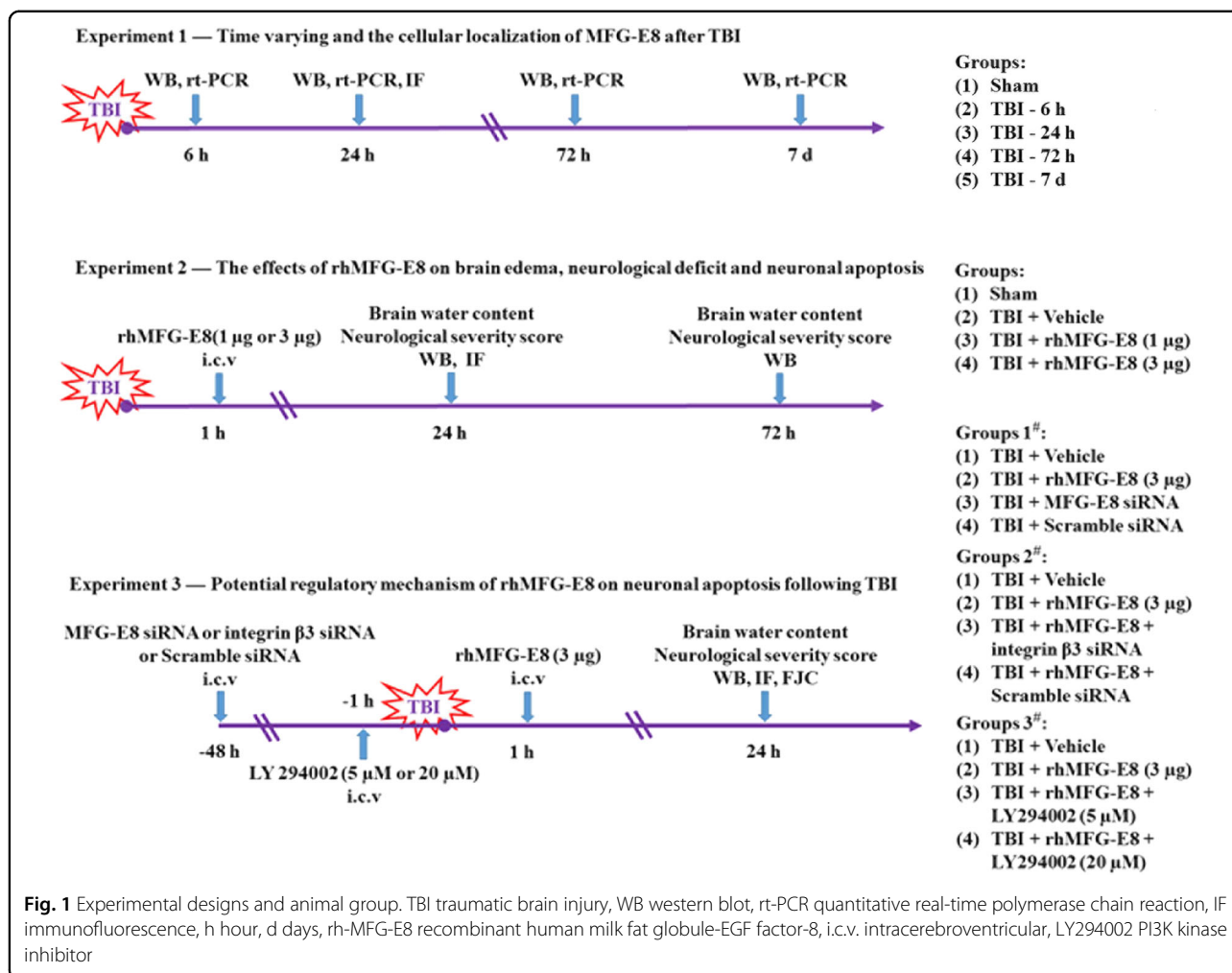
Experimental design

All rats were randomly assigned to the following experiments as described (Fig. 1).

Experiment design 1—To examine the expression of MFG-E8 in the cortex of rats after TBI. Rats were randomly assigned to five groups: Sham group and TBI group (6 h, 24 h, 72 h, 7 days) ($n = 9$ each). Six rats of each group were selected randomly for western blot analyses and quantitative real-time polymerase chain reaction and the rest rats for double-immunofluorescence staining.

Experiment design 2—To determine the effect of rhMFG-E8 on second brain injury after TBI. Rats were randomly assigned to four groups: Sham group, TBI + Vehicle group, TBI + rhMFG-E8 (1 and 3 μg) ($n = 15$ each). Assessment method including brain water content, neurological severity score, western blot analyses, and double-immunofluorescence staining.

Experiment design 3—To explore the potential mechanism of rhMFG-E8 on neuroprotection after TBI. Rats were randomly assigned into the following group: TBI + Vehicle group, TBI + rhMFG-E8, TBI + MFG-E8 siRNA, TBI + Scramble siRNA, TBI + rhMFG-E8 + integrin β_3 siRNA, TBI + rhMFG-E8 + Scramble siRNA, TBI + rhMFG-E8 + LY294002 (5 and 20 μM). Assessment method including western blot analyses and double-immunofluorescence staining, brain water content, neurological severity score, and Fluoro-Jade C (FJC) staining.



Intracerebroventricular administration

Intracerebroventricular (i.c.v.) drug administration was performed as previously described^{21,22}. Briefly, rats were placed in a stereotaxic frame after intraperitoneal anesthesia with sodium pentobarbital (50 mg/kg). The needle of a 10-μl Hamilton syringe (Shanghai Gaoge Industry & Trade Co., Ltd., Shanghai, China) was inserted into the right lateral ventricle through a burr hole using the following coordinates: 0.8 mm posterior and 1.5 mm lateral to the bregma, and 3.7 mm below the dural layer. rhMFG-E8 was purchased from R&D Systems, Inc. (McKinley, NE, USA) and injected at 1 h after TBI induction, doses of rhMFG-E8 were determined according to previous study^{18,23}. LY294002 (Sigma-Aldrich, USA, 5 and 20 μM) was dissolved in a sterile saline solution containing 1% dimethyl sulfoxide (DMSO) and injected at 1 h before TBI induction. According to the detection of siRNA effect and previous study¹⁸, MFG-E8 siRNA, integrin β3 siRNA, and scramble siRNA (500 pmol/3 μl, Santa Cruz Biotechnology) were injected into the right lateral ventricles at a rate of 0.5 μl/min with a 10-μl Hamilton syringe at 2 days before TBI induction.

Immunofluorescence staining

Immunofluorescence staining was performed as previously described²⁴. Briefly, the immunostaining protocol was as follows: rats were deeply euthanized and perfused with 4% paraformaldehyde in 0.1 mM phosphate-buffered saline (PBS, pH 7.4). Brain samples were immersed in 30% sucrose until sinking to the bottom. 8 μm-thick slices were cut with a cryostat. The slices of each coronal sections were incubated in blocking buffer for 2 h, then washed with PBS three times for 10 min. Next, the slices were incubated with anti-MFG-E8 (1:200) and anti-cleaved caspase-3 antibody (1:100) respectively, in a dark place overnight at 4 °C. Afterwards, the slices were washed three times with PBS and incubated with another antibody, namely anti-NeuN (1:100), anti-GFAP (1:100), anti-Iba-1 (1:50), under similar conditions. The following day, the slices were thoroughly washed with PBS and incubated with the corresponding secondary antibodies for 1 h. After the wash with PBS, the slices were stained with DAPI for 2 min to show the location of the nucleus. Coverslips were applied with mounting media. The

fluorescently-stained cells were imaged on an Olympus IX71 inverted microscope system and analyzed using the Image-Pro Plus 6.0 software (Media Cybernetics, Silver Spring, MD, USA). All of the processes were conducted by two investigators who were blinded to the grouping.

Western blot analysis

Western blot analysis was performed as previously described^{25,26}. Briefly, the total protein concentration of the lysate was determined by the Bradford method using the Bradford Protein Assay Kit (Beyotime Biotechnology, Shanghai, China). Equal amounts of proteins were resolved on a 10–12% sodium dodecyl sulfate-polyacrylamide gel electrophoresis (SDS-PAGE) gel and transferred onto polyvinylidene fluoride (PVDF) membrane (Immobilon-P, Millipore, Billerica, MA, USA). The membrane was blocked with 5% non-fat dry milk in TBST (Tris-buffered saline with 0.05% Tween 20) for 2 h at room temperature, and then incubated overnight at 4 °C, separately with the appropriate primary antibodies against the specific proteins. Specifically, MFG-E8 (Santa Cruz Biotechnology, USA, 1:200), AQP4 (Santa Cruz Biotechnology, USA, 1:200), Integrin β 3 (Santa Cruz Biotechnology, USA, 1:200), p-FAK (Cell Signaling Technology, USA, 1:1000), FAK (Cell Signaling Technology, USA, 1:1000), p-AKT (Cell Signaling Technology, USA, 1:1000), AKT (Cell Signaling Technology, USA, 1:1000), caspase-3 (Cell Signaling Technology, USA, 1:1000), Bcl-2 (Cell Signaling Technology, USA, 1:1000), Bax (Abcam, Cambridge, UK, 1:200), and β -actin (Bioworld Technology, USA, 1:5000) in a blocking buffer. Afterwards, the membrane was washed three times with TBST for 15 min, and then incubated with the secondary antibodies, namely HRP conjugated secondary antibodies (goat; Bioworld Technology, USA, 1:5000) or HRP conjugated secondary antibodies (horse; Cell Signaling Technology, USA, 1:1000) for 2 h at room temperature. Finally, following a 20-min wash with TBST, the protein bands were visualized via enhanced chemiluminescence (ECL) (Millipore, Billerica, MA, USA) and exposure to X-ray film. The western blot results were

analyzed using Un-Scan-It 6.1 software (Silk Scientific Inc., Orem, UT, USA).

Quantitative real-time polymerase chain reaction

Total RNA was extracted from tissues using Trizol reagent (Invitrogen Life Technologies, Carlsbad, CA, USA). RNA quality was insured by gel visualization and spectrophotometric analysis (OD260/280). After reverse transcription, quantitative analysis of the MFG-E8, Integrin β 3, IL-1 β , IL-6, and IL-10 mRNA expression were performed with the real-time PCR method²⁴ and the primers were synthesized by ShineGene Biotechnology (Shanghai, China) (Table 1). Test cDNA results were normalized to β -actin. All samples were analyzed in triplicate.

Terminal deoxynucleotidyl transferase dUTP nick end-labeling (TUNEL) staining

The brain tissue sections were examined for apoptotic cells using a terminal deoxynucleotidyl transferase dUTP nick end-labeling (TUNEL) detection kit (Roche, South San Francisco, CA, USA) following the manufacturer's instructions. Briefly, the sections were incubated with the TUNEL reagent for 1 h at 37 °C. The sections were then washed three times in PBS, counterstained with DAPI for 2 min, and rinsed with PBS. Coverslips were applied with mounting media. Fluorescence was imaged on an Olympus IX71 inverted microscope system. The number of apoptotic cells to DAPI stained-cells was regarded as apoptotic index (apoptotic cells/DAPI). Six random vision fields (40 \times) surrounding contusion in each coronal section were chosen, and the mean number of apoptotic index in the six views was regarded as the data of each section. A total of four sections from each animal were used for quantification. The final average number of the four sections was regarded as the data for each sample. Data are presented as the mean number of apoptotic index per 40 \times magnification field. All the processes were conducted by two investigators who were blinded to the grouping.

Table 1 Polymerase chain reaction (PCR) primer sequences

Target gene	Forward (5' to 3')	Reverse (5' to 3')
MFG-E8	CGGGCCAAGACAATGACATC	TCTCTCAGTCTCATTGCACACAAG
Integrin β 3	CGTCAGCCTTTACCAGAATTATAGTG	TTTCCCGTAAGCATCAACAATG
β -Actin	CGTGAAAAGATGACCCAGATCA	CACAGCCTGGATGGCTACGTA
IL-1 β	AAGCCTCGTGCTGCGGACC	TGAGGCCCAAGGCCACAGG
IL-6	GAGACTTCCATCCAGTTGCCT	TGGGAGTGGTATCCTCTGTGA
IL-10	GGTTGCCAAGCCTTATCG A	ACCTGCTCCACTGCCTTGCT

Table 2 Neurological severity scores (NSS)

	Points
Motor tests	
Raising rat by the tail (normal = 0; maximum = 3)	
Flexion of forelimb	1
Flexion of hindlimb	1
Head moved >10° to vertical axis within 30 s	1
Placing rat on the floor (normal = 0; maximum = 3)	
Normal walk	0
Inability to walk straight	1
Circling toward the paretic side	2
Fall down to the paretic side	3
Sensory tests (normal = 0; maximum = 2)	
Placing test (visual and tactile test)	1
Proprioceptive test (deep sensation, pushing the paw against the table edge to stimulate limb muscles)	2
Beam balance tests (normal = 0; maximum = 6)	
Balances with steady posture	0
Grasps side of beam	1
Hugs the beam and one limb falls down from the beam	2
Hugs the beam and two limbs fall down from the beam, or spins on beam (>60 s)	3
Attempts to balance on the beam but falls off (>40 s)	4
Attempts to balance on the beam but falls off (>20 s)	5
Falls off: no attempt to balance or hang on to the beam (<20 s)	6
Reflexes absent and abnormal movements (normal = 0; maximum = 4)	
Pinna reflex (head shake when touching the auditory meatus)	1
Corneal reflex (eye blink when lightly touching the cornea with cotton)	1
Startle reflex (motor response to a brief noise from snapping a clipboard paper)	1
Seizures, myoclonus, myodystony	1
Maximum points	18

Fluoro-Jade C (FJC) staining

FJC staining (Merckmillipore, Germany) was performed according to the operation instructions and to detect degenerating neurons. Briefly, frozen sections were prepared, fixed, and immersed in a basic alcohol solution consisting of 1% sodium hydroxide in 80% ethanol for 5 min, then rinsed for 2 min each in 70% ethanol and distilled water, and then incubated in 0.06% potassium

permanganate solution for 10 min. Following a 1–2 min water rinse, the slices were transferred for 10 min to a 0.0001% solution of FJC dissolved in 0.1% acetic acid vehicle and then rinsed through three changes of distilled water for 1 min per change. The slices were air-dried, coverslips were applied, and the sections were visualized on an Image J software (Image J 1.4, NIH, USA). Two observers blinded to the experimental group counted the FJC-positive cells in six sections per brain (at 40× magnification) through the injury's epicenter. The data were presented by the average number of FJC-positive neurons in the fields.

Brain water content

Brain water content was measured as previously studied²⁷. Animals were anesthetized with sodium pentobarbital (50 mg/kg; i.p.) and the brains were quickly dissected at 24 and 72 h after TBI. The brainstem was discarded, while the tissue of ipsilateral cortex, the contralateral cortex, and the cerebellum were harvested. The wet weight of each cortical tissue was measured, then dried for 72 h at 80 °C and the dry weight determined. All experiments were conducted by two investigators who were blinded to the grouping. The percentage of brain water content was calculated using the following formula: $=[(\text{wet weight} - \text{dry weight}) / \text{wet weight}] \times 100\%$.

Neurologic scoring

The neurological function of all rats before TBI and at 24 and 72 h after TBI were evaluated, according to previous studies^{28,29}, by three investigators who were blinded to the experimental groups. The grading of neurological severity scoring (NSS) was as follows: severe injury (score: 13–18); moderate injury (score: 7–12); mild injury (score: 1–6); no injury (score: 0) (Table 2).

Statistical analysis

The SPSS 17.0 software package was used for the statistical analysis. All data are expressed as the mean \pm standard deviation (SD). Comparisons between two groups were performed using Student's *t* test and multiple comparisons were performed using a one-way ANOVA followed by Tukey's test. A *P* value of <0.05 was regarded as statistically significant.

Results

General observations and mortality rate

Out of the 236 surgeries in rats that were performed, 12 rats died due to overdose anesthesia or serious injury in the TBI group. No rats died in Sham group 0% (0/12), and the overall mortality rate of TBI in rats was 5.08% (Fig. 2). There was no statistical difference in body weight and body temperature in any of the experimental groups (data not shown).

Groups		Mortality Rate
Experiment 1		
(1) Sham		0 (0/6)
(2) TBI - 6 h		0 (0/9)
(3) TBI - 24 h		0 (0/9)
(4) TBI - 72 h		0 (0/9)
(5) TBI - 7 d		10% (1/10)
Experiment 2		
(1) Sham	(n = 6)	0 (0/6)
(2) TBI + Vehicle	(n = 15)	6.25% (1/16)
(3) TBI + rhMFG-E8 (1 µg)	(n = 15)	11.76% (2/17)
(4) TBI + rhMFG-E8 (3 µg)	(n = 15)	11.76% (2/17)
Experiment 3		
Groups 1[#]:		
(1) TBI + Vehicle	(n = 8)	0 (0/8)
(2) TBI + rhMFG-E8 (3 µg)	(n = 12)	7.69% (1/13)
(3) TBI + MFG-E8 siRNA	(n = 12)	0 (0/12)
(4) TBI + Scramble siRNA	(n = 12)	0 (0/12)
Groups 2[#]:		
(1) TBI + Vehicle	(n = 8)	0 (0/8)
(2) TBI + rhMFG-E8 (3 µg)	(n = 18)	10% (2/20)
(3) TBI + rhMFG-E8 + integrin β3 siRNA	(n = 18)	0 (0/18)
(4) TBI + rhMFG-E8 + Scramble siRNA	(n = 18)	5.56% (1/18)
Groups 3[#]:		
(1) TBI + Vehicle	(n = 8)	0 (0/8)
(2) TBI + rhMFG-E8 (3 µg)	(n = 18)	0% (0/18)
(3) TBI + rhMFG-E8 + LY294002 (5 µM)	(n = 18)	5.26% (1/19)
(4) TBI + rhMFG-E8 + LY294002 (20 µM)	(n = 18)	5.26% (1/19)
Total		
Sham		0 (0/12)
TBI		5.08% (12/236)

Fig. 2 Mortality rate and general observations

Increased MFG-E8 expression peaks 24 h after TBI and is mainly expressed in microglia

To determine the role of MFG-E8 in rats after TBI, we first studied the expression and cellular localization of MFG-E8 in left cerebral cortical tissues. MFG-E8 protein and gene expression were examined by western blot analysis and quantitative real-time PCR, respectively. Following TBI, MFG-E8 protein expression was significantly increased at the 6 h time point, reaching its highest levels at 24 h and lasting up to 7 days (Fig. 3b, c). mRNA expression showed a similar pattern. MFG-E8 mRNA levels in the TBI group at the 24 h time point increased 50% relative to the mRNA levels in the Sham group (Fig. 3d). To determine the cellular localization of

MFG-E8 in damaged cortical tissues, we conducted double-immunofluorescence staining. MFG-E8 was found to locate exclusively to the cytoplasm and was primarily expressed in microglial cells with minimal expression in neurons. MFG-E8 was rarely expressed in astrocytes.

rhMFG-E8 decreased brain water content and improved neurological function after TBI in rats

To investigate the neuroprotective effects of MFG-E8 after TBI in rats, two different dosages of rhMFG-E8 (1 and 3 µg) were administered after a TBI event. Brain water content and neurological severity scores were used to evaluate brain edema and neurological function, respectively. The results showed that for both dosages of

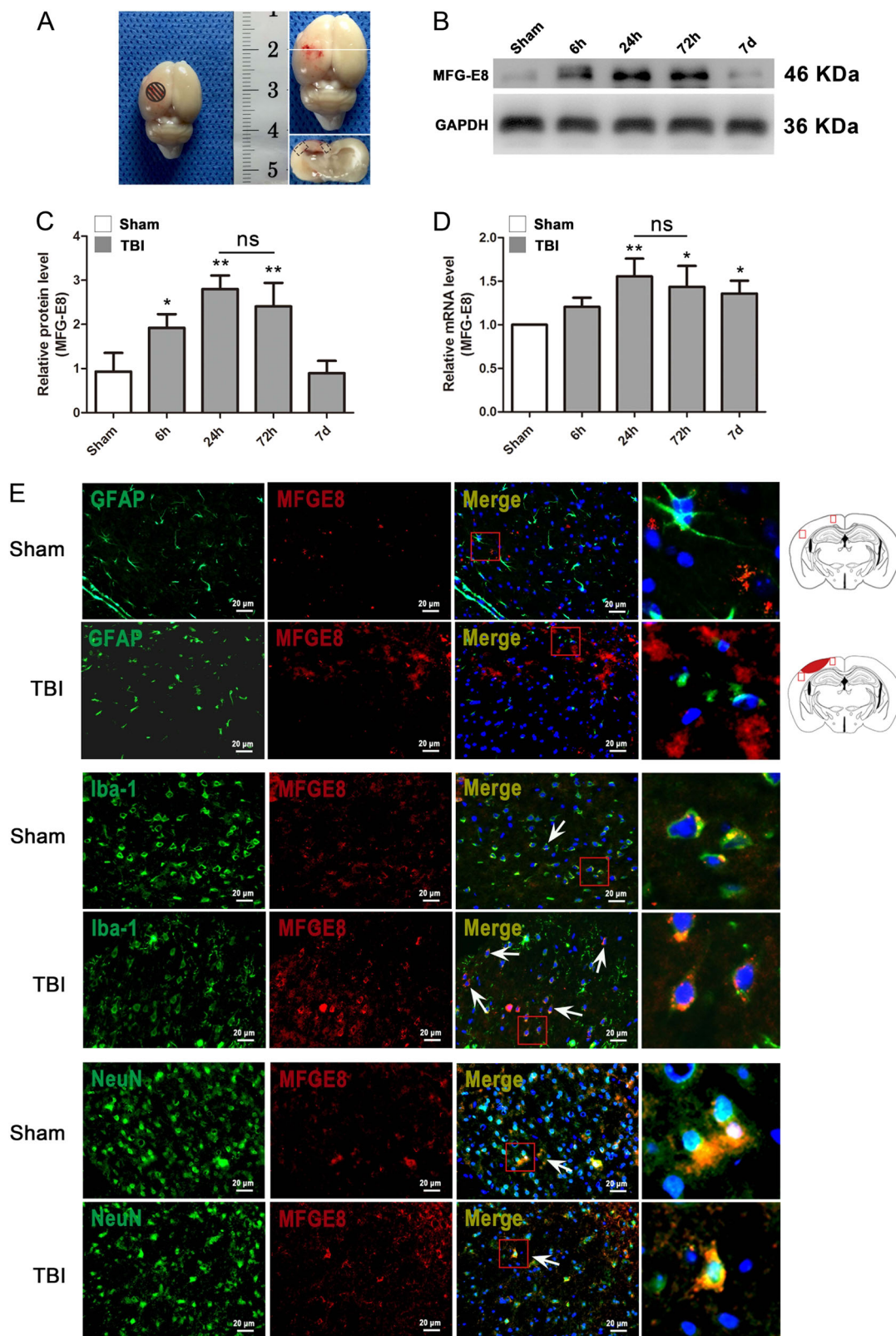


Fig. 3 (See legend on next page.)

(see figure on previous page)

Fig. 3 The expression of MFG-E8 on the mRNA and protein level and its cellular distribution after TBI. Experimental TBI model in SD rats and the tissue around the lesion in cortex was sampled for western blot and quantitative real-time PCR analysis in this study (a). The mRNA and protein expressions of MFG-E8 were measured at 6 h, 24 h, 72 h, and 7 days after TBI using western blotting and quantitative real-time PCR (b). The mRNA and protein expressions of MFG-E8 were significantly increased at 24 and 72 h after TBI as compared with the Sham group (c, d). Representative immunofluorescence co-staining images of MFG-E8/GFAP, MFG-E8/Iba-1, MFG-E8/NeuN in the Sham group and TBI group (24 h). Astrocytes, microglial cells, and neuron cells are labeled with GFAP (green), Iba-1 (green), and NeuN (green), respectively. (MFG-E8 = red, DAPI = blue). Diagram of coronal rat brain section showing the location of lesion cavity (red) and photograph region (red squares). The quantitative data are the mean \pm SD ($n = 9$ each; * $P < 0.05$; ** $P < 0.01$ vs. Sham group; ^{ns} $P > 0.05$). Bar = 20 μ m

rhMFG-E8, brain water content decreased in the ipsilateral cortex compared with the TBI + Vehicle control group at 24 and 72 h (Fig. 4a, c). Administration of 1 μ g rhMFG-E8 did not improve the neurological deficits at 24 and 72 h, whereas 3 μ g rhMFG-E8 significantly affected neurological function at 24 and 72 h post-TBI (Fig. 4b, d). Furthermore, the neurological severity scores in the TBI + rhMFG-E8 (3 μ g) group decreased 33.33% relative to TBI + Vehicle group at 24 h and 32.83% at 72 h. This suggests treatment with 3 μ g rhMFG-E8 at 24 h after TBI provides more effective neuroprotection. Accordingly, the high rhMFG-E8 dosage (3 μ g) and most effective treatment time (24 h) were chosen for all subsequent mechanistic experiments, and the negative controls of rhMFG-E8 were also provided (Supplementary Figure 1).

The effect of rhMFG-E8 on AQP4 expression, a protein that plays a key role in the brain edema process, was also assessed after TBI through western blot analysis and immunofluorescence staining. AQP4 protein levels were significantly increased in the TBI + Vehicle group compared with the Sham group, while rhMFG-E8 treatment reversed AQP4 expression, with a high rhMFG-E8 dosage being more effective (Fig. 4e, f).

Administration of rhMFG-E8 reduces neuronal apoptosis at 24 h after TBI in rats

Neuronal apoptosis plays an important role in the pathogenesis of the secondary insult following TBI. To investigate the potential role of MFG-E8 after TBI in rats, we first examined the protein levels of the apoptosis indicators, cleaved caspase-3 and Bcl-2, via western blot analysis. Following TBI, the levels of the pro-apoptosis protein cleaved caspase-3 were significantly increased, while the anti-apoptosis protein Bcl-2 was markedly decreased in the TBI + Vehicle group compared with the Sham group at both 24 and 72 h (Fig. 5a–f). By contrast, the expression of cleaved caspase-3 and Bcl-2 were reversed in TBI + rhMFG-E8 group relative to the TBI + Vehicle group. Treatment with rhMFG-E8 at 24 h after TBI also provided a more marked effect than at 72 h (Fig. 5a–f).

TUNEL immunofluorescence staining was also used to evaluate the role of rhMFG-E8 in anti-apoptosis after TBI. The results showed that the number of TUNEL-positive

neurons in TBI + Vehicle group were significantly increased compared to the Sham group, while administration of rhMFG-E8 reduced the amount of TUNEL-positive neurons at 24 h post-TBI (Fig. 5g, h).

To further verify the anti-apoptosis effect of rhMFG-E8, we administrated MFG-E8 siRNA treatment. Treatment with rhMFG-E8 markedly increased MFG-E8 protein expression compared with the TBI + Vehicle group, while MFG-E8 siRNA treatment significantly decreased MFG-E8 protein levels at 24 h following TBI (Fig. 6a, b). Similarly, the levels of pro-apoptosis-associated proteins in TBI + rhMFG-E8 group, such as cleaved caspase-3 and Bax, were significantly down-regulated relative to the TBI + Vehicle group, while the expression of pro-survival protein Bcl-2 was up-regulated (Fig. 6a, c–e). After treatment with MFG-E8 siRNA, the levels of apoptosis-associated proteins were reversed compared with the TBI + rhMFG-E8 group (Fig. 6a, c–e). We also used double-immunofluorescence staining to evaluate the role of rhMFG-E8 on neuronal apoptosis. The number of cleaved caspase-3 positive-neurons in TBI + rhMFG-E8 group were significantly decreased relative to the TBI + Vehicle group, while they were increased after MFG-E8 siRNA treatment (Fig. 6f, g).

Integrin- β 3 knockdown and PI3K inhibition abolish the anti-apoptosis effect of rhMFG-E8 at 24 h after TBI

To investigate the regulatory mechanism of rhMFG-E8 on apoptosis, integrin- β 3 siRNA was used. The inhibitory effect of integrin- β 3 siRNA was first examined via western blot analysis. Integrin- β 3 expression showed no statistical difference between the TBI + Vehicle group and TBI + rhMFG-E8 group, while it was significantly decreased following treatment with integrin- β 3 siRNA (Fig. 7a). Subsequently, the levels of integrin- β 3/FAK/AKT pathway-associated proteins were assessed by western blot. The expression of p-FAK and p-AKT in the TBI + rhMFG-E8 group were markedly increased compared with the TBI + Vehicle group, while integrin- β 3 siRNA treatment significantly inhibited the effect of rhMFG-E8 on p-FAK and p-AKT (Fig. 7b, c). In the TBI + rhMFG-E8 group, pro-survival protein Bcl-2 expression was up-regulated, whereas pro-apoptosis-associated protein cleaved caspase-3 and Bax were down-regulated.

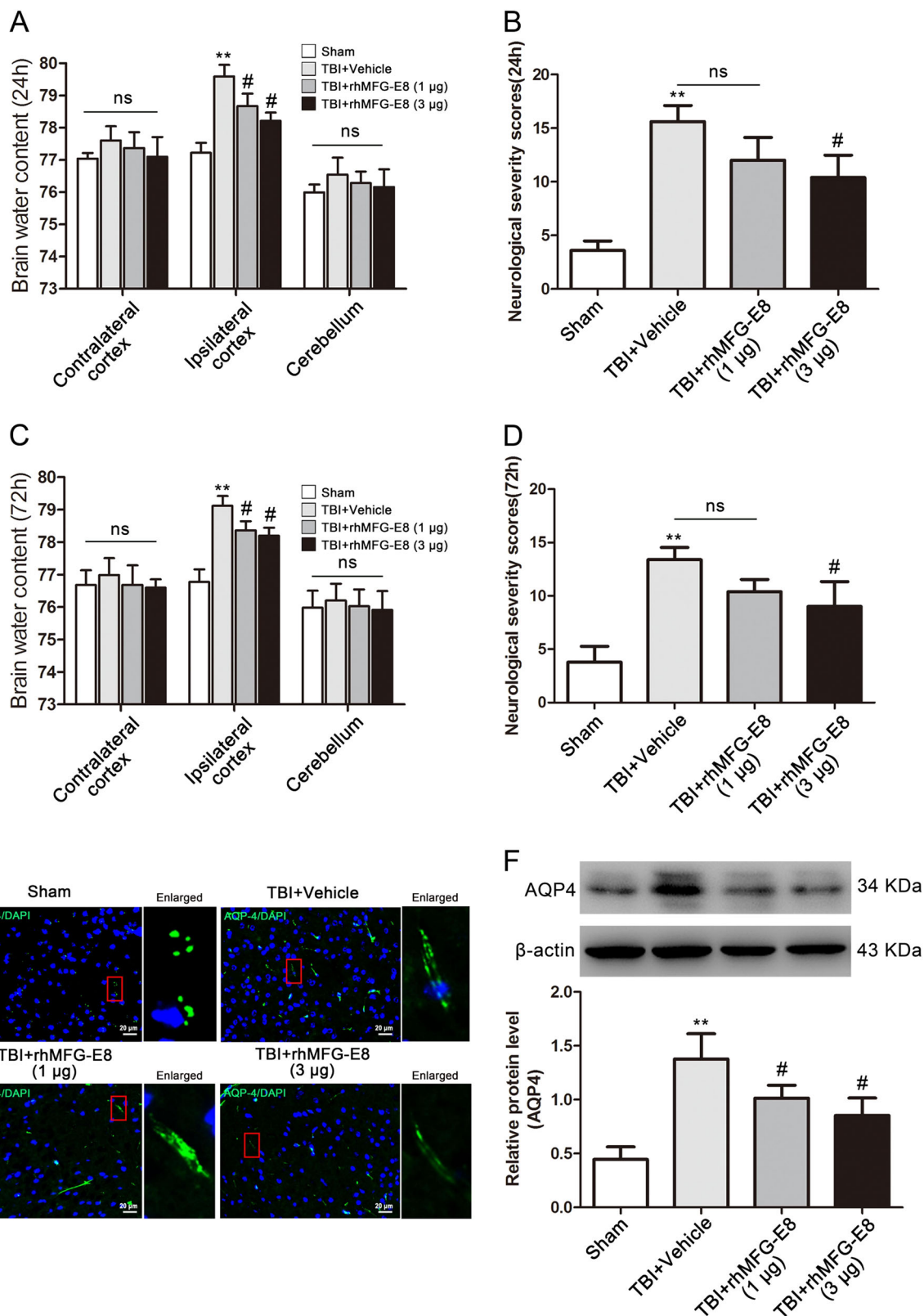


Fig. 4 (See legend on next page.)

(see figure on previous page)

Fig. 4 The effect of rhMFG-E8 on neuroprotection was evaluated by brain water content, neurological severity scores at 24 and 72 h after TBI. Both two dosages of rhMFG-E8 decreased brain edema in the ipsilateral cortex at 24 and 72 h after TBI (a, c), while only high dosage of rhMFG-E8 on neurological function has statistical differences compared with the TBI + Vehicle group at 24 and 72 h post-TBI (b, d). Representative immunofluorescence staining images of AQP4/DAPI (AQP4 = green, DAPI = blue) (e). Western blotting showed that administration of rhMFG-E8 decreased the expression of AQP-4 as compared with the TBI + Vehicle group at 24 h after TBI (f). The quantitative data are the mean ± SD (n = 15 each; **P < 0.01 vs. Sham group; #P < 0.05 vs. TBI + Vehicle group; ^{ns}P > 0.05). Bar = 20 μm

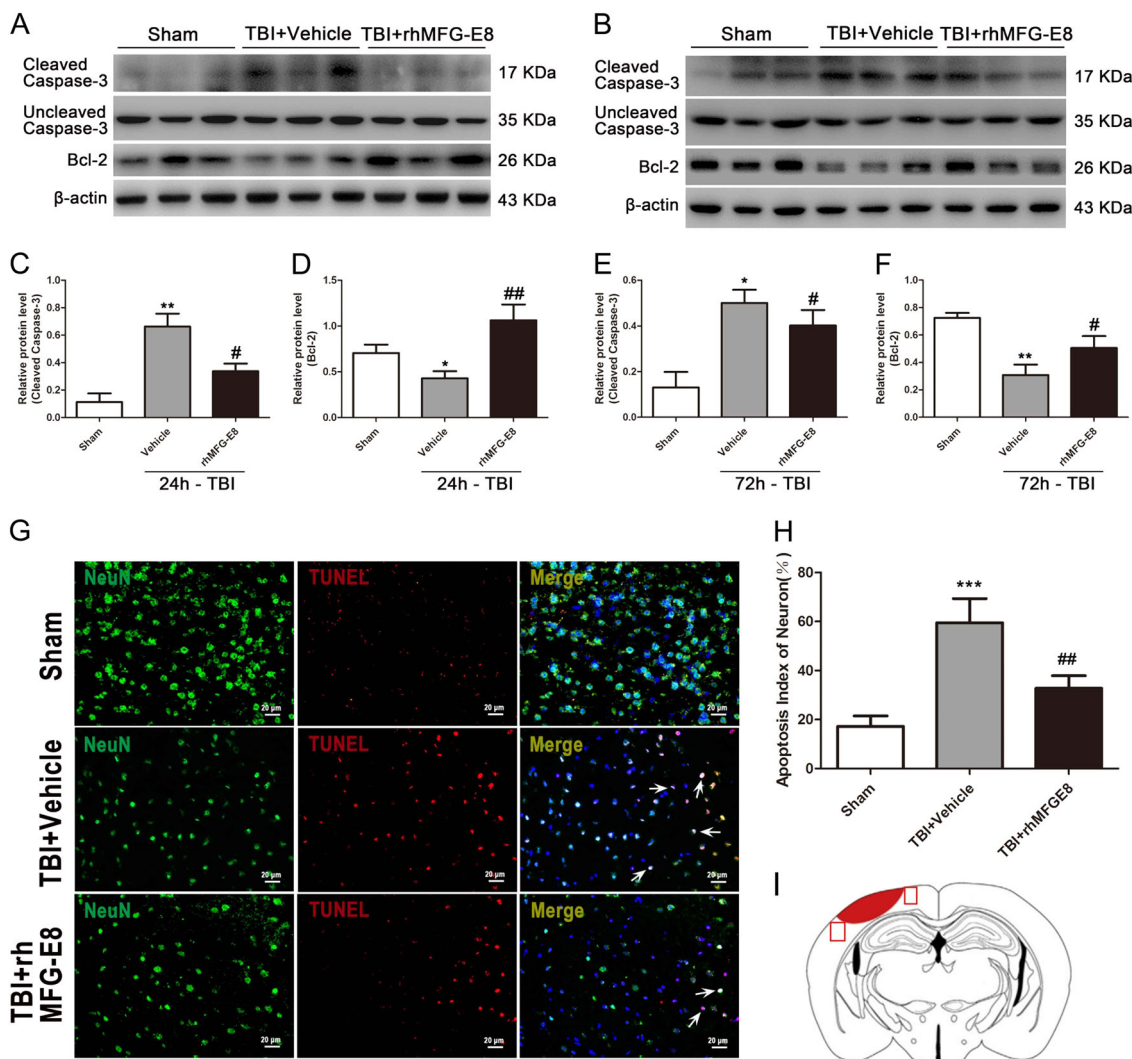
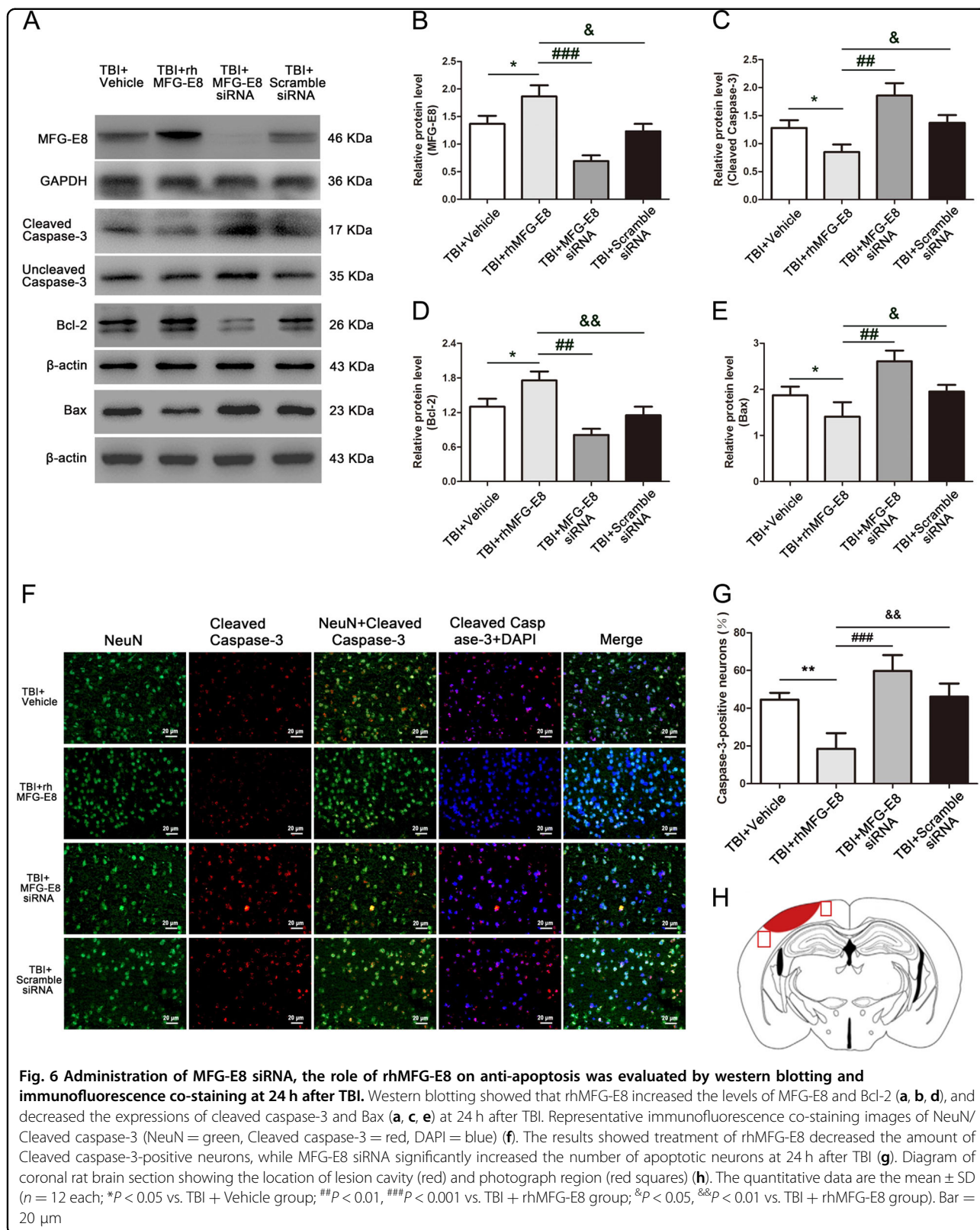


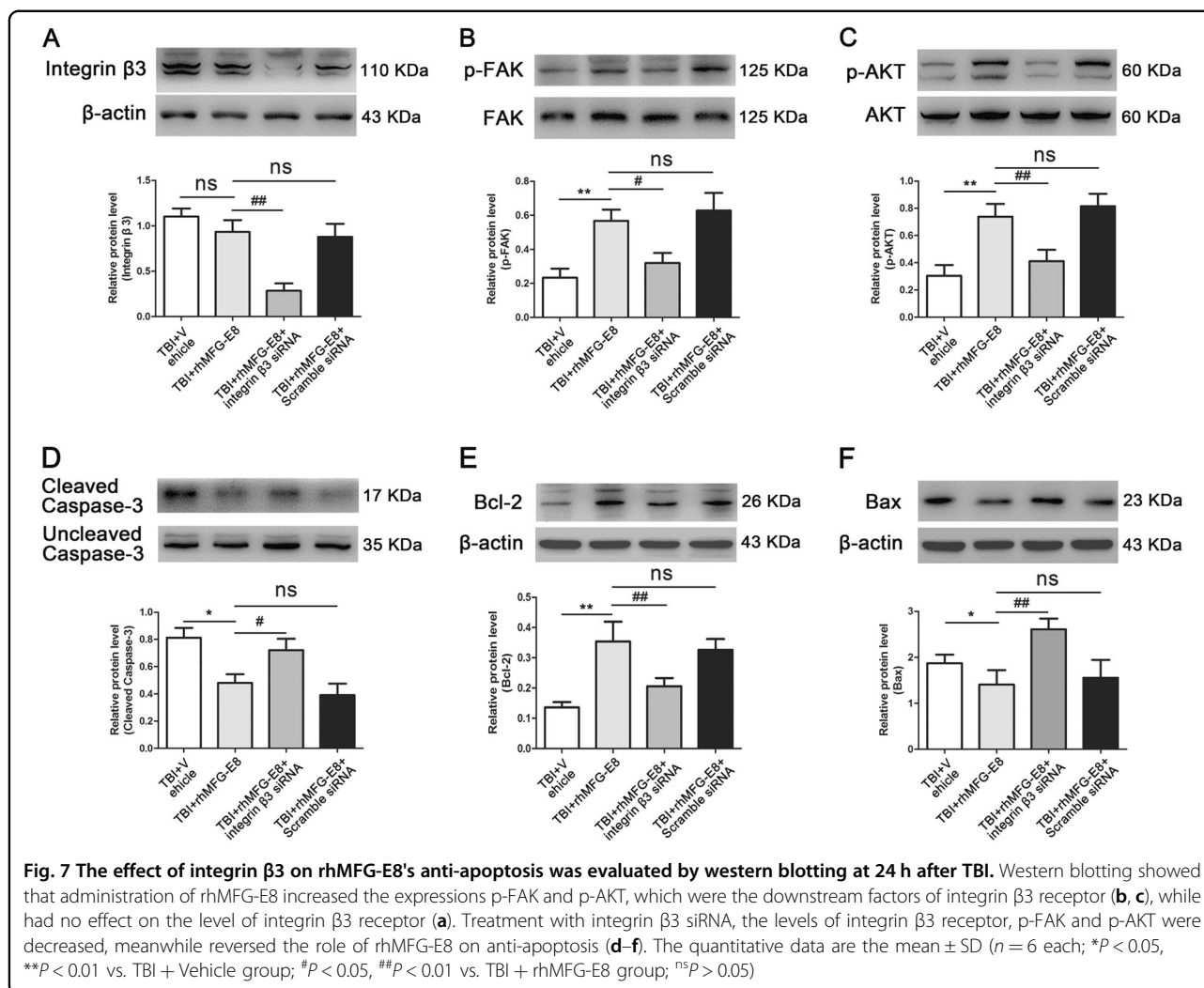
Fig. 5 The effect of rhMFG-E8 on neuronal apoptosis was evaluated by western blotting and immunofluorescence co-staining at 24 and 72 h after TBI. Western blotting showed that rhMFG-E8 (3 μg) administration decreased the expression of cleaved caspase-3 and increased the expression of Bcl-2 at 24 and 72 h after TBI (a–f). Representative immunofluorescence staining images of NeuN/DAPI (NeuN = green, TUNEL = red) (g), results showed administration of rhMFG-E8 decreased the amount of TUNEL-positive neurons at 24 h after TBI (h). Diagram of coronal rat brain section showing the location of lesion cavity (red) and photograph region (red squares) (i). The quantitative data are the mean ± SD (n = 15 each; *P < 0.05, **P < 0.01 vs. Sham group; **P < 0.01 vs. TBI + Vehicle group; #P < 0.05, ##P < 0.01 vs. TBI + Vehicle group). Bar = 20 μm

Treatment with integrin-β3 siRNA abolished these effects (Fig. 7d–f).

Two dosages of PI3K inhibitor LY294002 (5 and 20 μM) were also evaluated. Western blot analysis revealed a

significant decrease of p-AKT in the TBI + rhMFG-E8 + LY294002 group, with the higher dose of LY294002 providing a stronger effect (Fig. 8a, b). However, PI3K inhibitor LY294002 (5 and 20 μM) had no effect on the





protein levels of integrin-β3 and p-FAK compared with the TBI + rhMFG-E8 group (Fig. 8a, c, d). In addition, the levels of cleaved caspase-3 and Bax were increased, while Bcl-2 decreased in the TBI + rhMFG-E8 + LY294002 group as compared with the TBI + rhMFG-E8 group. High doses of LY294002 exhibited a more pronounced effect on cleaved caspase-3, Bax, and Bcl-2 expression after rhMFG-E8 administration (Fig. 8e–h). Meanwhile, the percentage of cleaved caspase-3 positive-neurons in the TBI + rhMFG-E8 group were significantly decreased compared with the TBI + Vehicle group, whereas they were elevated by integrin-β3 siRNA or LY294002 (5 and 20 μM) treatment (Fig. 9a, b).

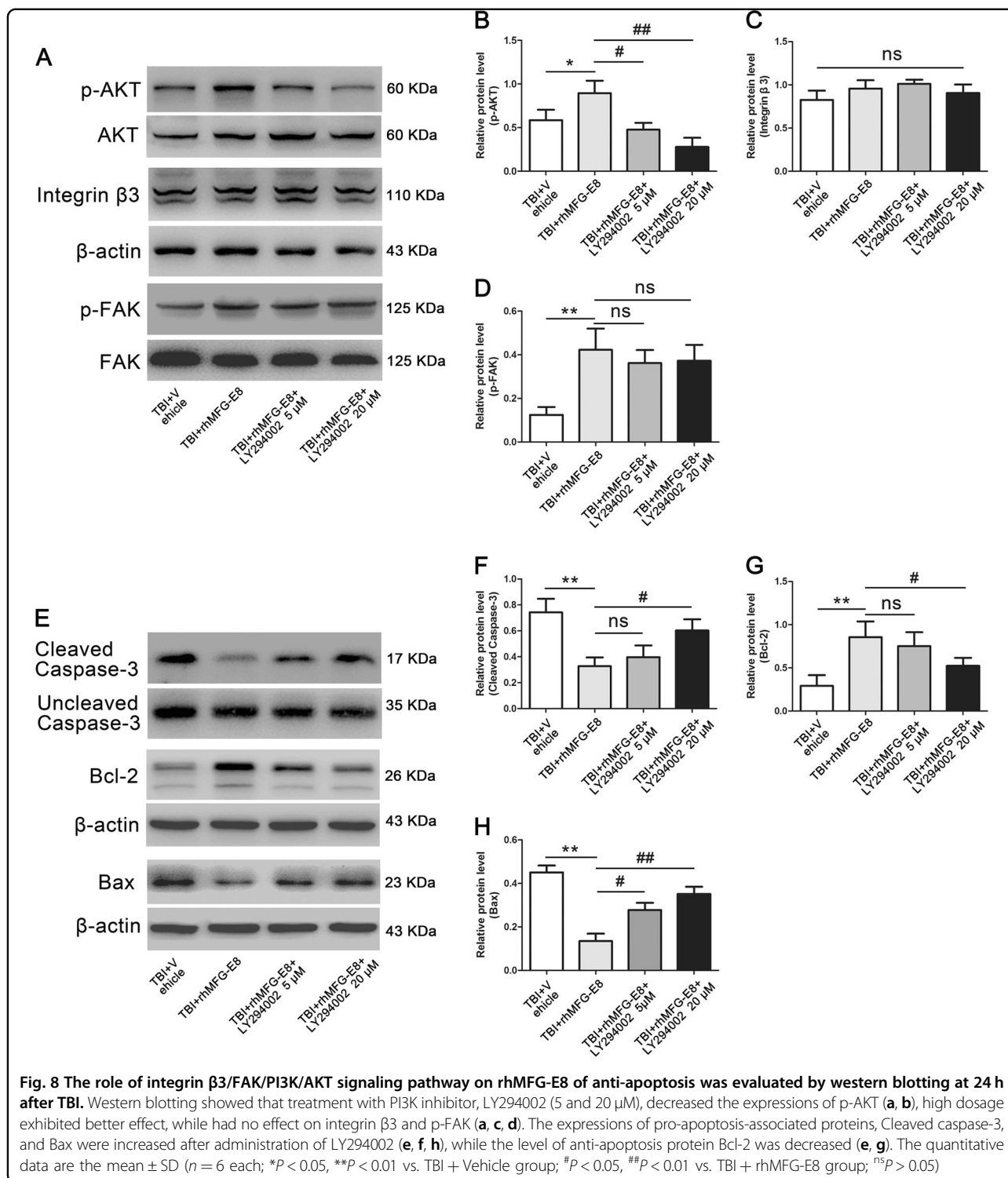
MFG-E8 provides beneficial effects dependent on the integrin-β3/FAK/PI3K/AKT signaling pathway

Brain water content, neurological severity scores, and FJC staining were examined to evaluate the potential mechanisms of rhMFG-E8. We used integrin-β3 siRNA and PI3K inhibitor LY294002 (5 and 20 μM) to

demonstrate whether the integrin-β3/FAK/PI3K/AKT signaling pathway participates in MFG-E8-induced neuroprotection. As shown in Fig. 10a, b, the number of FJC-positive cells in the ipsilateral cortex notably declined in the TBI + rhMFG-E8 group relative to the TBI + Vehicle group, whereas they increased in the TBI + rhMFG-E8 + integrin β3 siRNA and TBI + rhMFG-E8 + LY294002 (5 and 20 μM) groups. In addition, brain water content in the ipsilateral cortex and neurological severity scores decreased in the TBI + rhMFG-E8 (3 μg) group compared with the TBI + Vehicle group at 24 h after TBI, whereas they increased after administration of integrin β3 siRNA and PI3K inhibitor LY294002. However, no statistical difference was observed between the TBI + rhMFG-E8 and TBI + rhMFG-E8 + LY294002 (5 and 20 μM) groups (Fig. 10d, e).

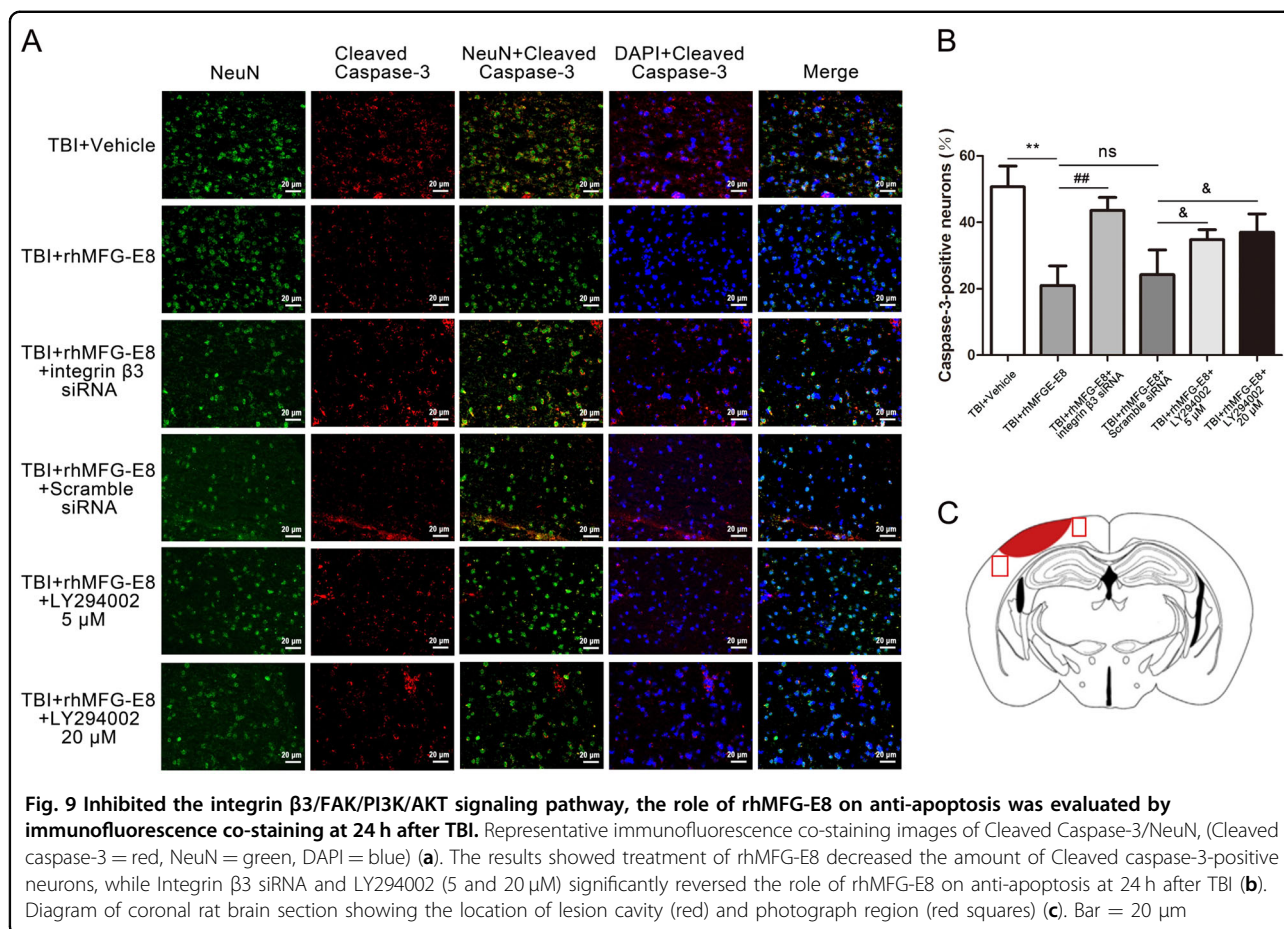
Discussion

This study presents the link between MFG-E8 and the integrin-β3/FAK/PI3K/AKT signaling pathway, both of



which provide neuroprotection following TBI in rats. MFG-E8 was primarily located in microglia and neurons, and showed increased expression in the early stages of TBI. Treatment with rhMFG-E8 markedly alleviated TBI-induced brain edema and neurological deficits following TBI. Meanwhile, rhMFG-E8 treatment up-regulated the

expression of integrin- β 3/FAK/PI3K/AKT signaling pathway components, and decreased neuronal apoptosis after TBI. In contrast, integrin- β 3 knockdown by siRNA and PI3K inhibitor LY294002 treatment abolished the effect of rhMFG-E8 on anti-apoptosis and neuroprotection. MFG-E8 is suggested to provide neuroprotection



through modulation of the integrin- β 3/FAK/PI3K/AKT signaling pathway, which may offer an attractive therapeutic target following TBI.

Increasing evidence points to the essential function of MFG-E8 in diverse physiological functions, including inflammation⁵, angiogenesis³⁰, clearance of apoptotic cells^{3,12}, and fertilization⁷. Several recent studies confirmed the therapeutic potential of MFG-E8 in various brain injury diseases, including neurodegenerative diseases^{8,11,31}, cerebral ischemic injury^{5,12}, and subarachnoid hemorrhage¹⁸. It has also been shown that MFG-E8 provides neuroprotection via suppressing inflammation and apoptosis, which may owe to the regulation of integrin-mediated cell adhesion and activation of the FAK-dependent phosphatidylinositol 3-kinase-AKT pathway^{12,17}. Similarly, using an ischemic cerebral injury rat model that was binge-treated with the integrin- β 3 receptor, MFG-E8 treatment reduced the infarct volume and accumulation of apoptotic cells, while simultaneously inhibiting the production of the inflammasome complex⁵. Liu et al. showed MFG-E8 was mainly expressed in macrophages and the levels of endogenous brain MFG-E8 increased in subarachnoid hemorrhage rats. In addition, exogenous rhMFG-E8 reduced brain edema and

improved neurological function through attenuation of oxidative stress¹⁸. All of these studies indicate that MFG-E8 is essential for neuroprotection. Our results demonstrated that exogenous rhMFG-E8 could alleviate TBI-induced brain edema and neurological deficits, potentially through the inhibition of neuronal apoptosis, which was consistent with previous studies^{18,32}. The effect of MFG-E8 on the reduction of brain edema might be through the modulation of the protein of AQP4. The previous study has shown that MFG-E8 could accelerate the tissue regeneration and neovascularization through modulation of VEGF-AKT signaling pathway⁶. Therefore, we supposed that the role of MFG-E8 on anti-brain edema might be bound up with VEGF-AKT pathway, not exclude the effect on the blood-brain barrier and its permeability. We will explore the mechanism of MFG-E8 on brain edema in the following experiments.

Apoptosis, as an important pathological process after TBI, can promote cell death through the triggering of devastating cascades³³. Briefly, this owes to the reciprocal activation of apoptosis-related proteins (such as Bax, Bcl-2, and cleaved caspase-3) and cytoplasmic organelle damage, which lead to apoptosis¹⁹. Thereafter, apoptotic cells induce an immune response and tissue injury

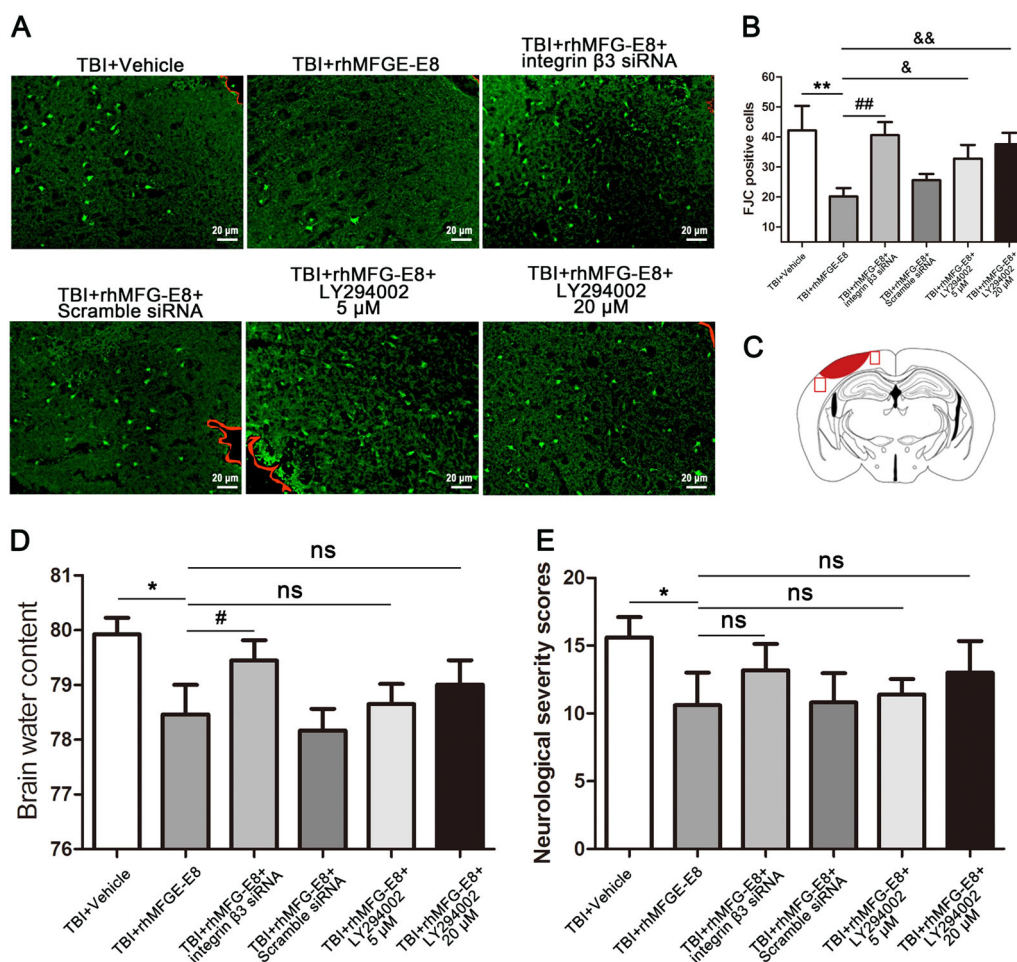


Fig. 10 Inhibited the integrin β /FAK/PI3K/AKT signaling pathway, the role of rhMFG-E8 on neuroprotection was evaluated by Fluoro-Jade C (FJC), brain water content, and neurological severity score at 24 h after TBI. Representative immunofluorescence staining images of FJC (green). The boundary of injury cortex was labeled by the red trajectory (a). The results showed treatment of rhMFG-E8 decreased the amount of FJC-positive cells, while increased it by Integrin β siRNA and LY294002 (5 and 20 μ M) at 24 h after TBI (b). Diagram of coronal rat brain section showing the location of lesion cavity (red) and photograph region (red squares) (c). Administration of rhMFG-E8 decreased brain edema in the ipsilateral cortex, meanwhile decreased the neurological severity score at 24 h after TBI, while integrin β siRNA and LY294002 (5 and 20 μ M) inverted the role of rhMFG-E8 on neuroprotection following TBI (d, e). The quantitative data are the mean \pm SD ($n = 6$ each; * $P < 0.05$, ** $P < 0.01$ vs. TBI + Vehicle group; # $P < 0.05$, ## $P < 0.01$ vs. TBI + rhMFG-E8 group; ns $P > 0.05$). Bar = 20 μ m

through the release of damage-associated molecular patterns (DAMPs)²¹. Meanwhile, previous studies have shown that the promotion of apoptotic cell removal was beneficial to various brain injury diseases^{12,34,35}. In addition, MFG-E8 was shown to exhibit the physiological effect during cell–cell interaction through its highly conserved arginine–glycine–aspartate (RGD) motif, which could recognize the receptors of $\alpha_v\beta_{3/5}$ -integrin in macrophage cells³. While, under pathologic conditions, it has been reported that MFG-E8 could target the apoptotic cells by binding phosphatidylserine (PS) and induce apoptotic cell phagocytosis via the $\alpha_v\beta_{3/5}$ -integrin receptor of phagocytes^{5,36}. Under neurodegenerative conditions, the MFG-E8 secreted from microglia could provide neuroprotection by enhancing oligomeric amyloid (α A β)

phagocytosis by microglia and reducing α A β -induced neuronal cell death¹¹. Whereas, the effect of MFG-E8 on TBI has not been previously investigated. In our study, we demonstrated that rhMFG-E8 inhibited neuronal apoptosis via $\alpha_v\beta_{3/5}$ -integrin receptor following TBI in rats, and, for the first time, we demonstrated the beneficial effect of rhMFG-E8 in TBI via regulation of apoptosis.

MFG-E8 modulated the expression of apoptosis-related proteins through its integrin $\alpha_v\beta_3$ receptor, leading us to focus on the potential underlying mechanism. A previous study showed that the FAK-AKT survival pathway could be activated via the $\alpha_v\beta_3$ integrin receptor and, through this pathway, elevated *bcl-2* gene transcription and the expression of anti-apoptotic protein Bcl-2¹⁷. Furthermore, the PI3K-AKT pathway has been confirmed to be

neuroprotective through modulation of apoptosis in various brain injury diseases, including TBI^{37,38}, neurodegenerative disease^{39,40}, and cerebral ischemia^{41,42}. We therefore speculated that the potential underlying mechanism of MFG-E8 on anti-apoptosis following TBI was through binding to the receptor of integrin- β 3 and activating its downstream FAK/PI3K/AKT signaling pathway. For this purpose, we examined the expression of integrin- β 3, FAK, and AKT. Treatment with rhMFG-E8 significantly increased p-FAK and p-AKT expression after TBI at 24 h, while integrin- β 3 knockdown abolished the effect of rhMFG-E8 on anti-apoptosis and FAK/PI3K/AKT pathway activation. To further define the role of MFG-E8 on the FAK/PI3K/AKT signaling pathway, we also evaluated the PI3K kinase inhibitor LY294002, which displayed similar effects to that of integrin- β 3 knockdown. The only difference was that LY294002 had no effect on the expression of integrin- β 3 and p-FAK. We therefore concluded that MFG-E8 inhibited neuronal apoptosis and improved neurological function of TBI, which appears to occur through modulation of the integrin- β 3/FAK/PI3K/AKT signaling pathway.

To the best of our knowledge, these results demonstrate for the first time the effect MFG-E8 has on integrin- β 3/FAK/PI3K/AKT signaling, via the modulation of apoptosis after TBI. However, our study had several limitations. First, we only used MFG-E8 siRNA, integrin β 3 siRNA, and LY294002 (PI3K kinase inhibitor), which might not have had an efficient inhibitor effect. Therefore, the data from gene knock-out rats (*mfg-e8*^{-/-} and *integrin β 3*^{-/-}) might be more persuasive. Second, we only examined the effect of MFG-E8 on integrin- β 3/FAK/PI3K/AKT pathway, additional MFG-E8 signaling pathways affecting apoptosis should be studied further.

Conclusion

MFG-E8 provides neuroprotection after TBI through inhibiting neuronal apoptosis, attenuating brain edema, and improving neurological function, while knocking down MFG-E8 and integrin β 3 via siRNA, or inhibiting the activation of PI3K by LY294002 abolished the effect of rhMFG-E8 on anti-apoptosis following TBI. It is suggested that MFG-E8 reduced apoptosis might depend on integrin β 3/FAK/PI3K/AKT pathway. Therefore, MFG-E8 might be a therapeutic target to improve neurological deficits and alleviate neuronal apoptosis after TBI.

Acknowledgements

The authors acknowledge the support for this research by grants from the National Natural Science Foundation of China (No. 81371294 for C.-H.H., No. 81401029 for W.L., and No. 81400980 for Z.Z.).

Author details

¹Department of Neurosurgery, The Affiliated Drum Tower Hospital, School of Medicine, Nanjing University, Zhongshan Road 321, Nanjing 210008 Jiangsu Province, PR China. ²Department of Neurosurgery, The First Affiliated Hospital of Wannan Medical College, Wuhu, Anhui Province, PR China. ³Department of

Neurosurgery, The Second Affiliated Hospital of Guangzhou Medical University, Guangzhou, Guangdong Province, PR China. ⁴Department of Neurosurgery, The Affiliated Drum Tower Hospital, Nanjing Medical University, Nanjing, Jiangsu Province, PR China

Author contributions

Y.-Y.G. designed the project, performed the TBI model and biochemical analysis, and wrote the manuscript. Z.-H.Z. provided the data of the animal studies and real-time polymerase chain reaction assay. Z.Z., Y.L., and Z.-n.Y. performed the immunofluorescence staining. X.-S.Z., C.-L.C., and L.-Y.W. provided the data of western blotting. W.L. and C.-H.H. contributed to the design and provided critical revisions. All authors participated in the revision of manuscript and approved the final article.

Conflict of interest

The authors declare that they have no conflict of interest.

Publisher's note

Springer Nature remains neutral with regard to jurisdictional claims in published maps and institutional affiliations.

Supplementary Information accompanies this paper at (<https://doi.org/10.1038/s41419-018-0939-5>).

Received: 3 March 2018 Revised: 8 July 2018 Accepted: 30 July 2018

Published online: 28 August 2018

References

- Kline, A. E., Leary, J. B., Radabaugh, H. L., Cheng, J. P. & Bondi, C. O. Combination therapies for neurobehavioral and cognitive recovery after experimental traumatic brain injury: is more better? *Prog. Neurobiol.* **142**, 45–67 (2016).
- Gyoneva, S. & Ransohoff, R. M. Inflammatory reaction after traumatic brain injury: therapeutic potential of targeting cell–cell communication by chemokines. *Trends Pharmacol. Sci.* **36**, 471–480 (2015).
- Aziz, M., Jacob, A., Matsuda, A. & Wang, P. Review: milk fat globule-EGF factor 8 expression, function and plausible signal transduction in resolving inflammation. *Apoptosis* **16**, 1077–1086 (2011).
- Carrascosa, C. et al. MFG-E8/lactadherin regulates cyclins D1/D3 expression and enhances the tumorigenic potential of mammary epithelial cells. *Oncogene* **31**, 1521–1532 (2012).
- Deroide, N. et al. MFG-E8 inhibits inflammasome-induced IL-1 β production and limits postischemic cerebral injury. *J. Clin. Invest.* **123**, 1176–1181 (2013).
- Silvestre, J. S. et al. Lactadherin promotes VEGF-dependent neovascularization. *Nat. Med.* **11**, 499–506 (2005).
- Ensslin, M. A. & Shur, B. D. Identification of mouse sperm SED1, a bimotif EGF repeat and discoidin-domain protein involved in sperm–egg binding. *Cell* **114**, 405–417 (2003).
- Raymond, A., Ensslin, M. A. & Shur, B. D. SED1/MFG-E8: a bi-motif protein that orchestrates diverse cellular interactions. *J. Cell. Biochem.* **106**, 957–966 (2009).
- Fuller, A. D. & Van Eldik, L. J. MFG-E8 regulates microglial phagocytosis of apoptotic neurons. *J. Neuroimmune Pharmacol.* **3**, 246–256 (2008).
- Kranich, J. et al. Engulfment of cerebral apoptotic bodies controls the course of prion disease in a mouse strain-dependent manner. *J. Exp. Med.* **207**, 2271–2281 (2010).
- Li, E. et al. The neuroprotective effects of milk fat globule-EGF factor 8 against oligomeric amyloid beta toxicity. *J. Neuroinflamm.* **9**, 148 (2012).
- Cheyuo, C. et al. Recombinant human MFG-E8 attenuates cerebral ischemic injury: its role in anti-inflammation and anti-apoptosis. *Neuropharmacology* **62**, 890–900 (2012).
- Hanayama, R. et al. Autoimmune disease and impaired uptake of apoptotic cells in MFG-E8-deficient mice. *Science* **304**, 1147–1150 (2004).
- Hanayama, R. et al. Identification of a factor that links apoptotic cells to phagocytes. *Nature* **417**, 182–187 (2002).
- Zhang, S. et al. MFG-E8, a clearance glycoprotein of apoptotic cells, as a new marker of disease severity in chronic obstructive pulmonary disease. *Braz. J. Med. Biol. Res.* **48**, 1032–1038 (2015).

16. Farrelly, N., Lee, Y. J., Oliver, J., Dive, C. & Streuli, C. H. Extracellular matrix regulates apoptosis in mammary epithelium through a control on insulin signaling. *J. Cell Biol.* **122**, 1337–1348 (1999).
17. Matter, M. L. & Ruoslahti, E. A signaling pathway from the alpha5beta1 and alpha(v)beta3 integrins that elevates bcl-2 transcription. *J. Biol. Chem.* **276**, 27757–27763 (2001).
18. Liu, F. et al. Recombinant milk fat globule-EGF factor-8 reduces oxidative stress via integrin β 3/nuclear factor erythroid 2-related factor 2/heme oxygenase pathway in subarachnoid hemorrhage rats. *Stroke* **45**, 3691–3697 (2014).
19. Wei, W. et al. Alpha lipoic acid inhibits neural apoptosis via a mitochondrial pathway in rats following traumatic brain injury. *Neurochem. Int.* **87**, 85–91 (2015).
20. Gao, Y. et al. Tetrahydrocurcumin reduces oxidative stress-induced apoptosis via the mitochondrial apoptotic pathway by modulating autophagy in rats after traumatic brain injury. *Am. J. Transl. Res.* **9**, 887–899 (2017).
21. Zhang, X. S. et al. Sirtuin 1 activation protects against early brain injury after experimental subarachnoid hemorrhage in rats. *Cell Death Dis.* **7**, e2416 (2016).
22. Wang, J. et al. Effects of crenolanib, a nonselective inhibitor of PDGFR, in a mouse model of transient middle cerebral artery occlusion. *Neuroscience* **364**, 202–211 (2017).
23. Shi, X. et al. MFG-E8 selectively inhibited A β -induced microglial M1 polarization via NF- κ B and PI3K-Akt pathways. *Mol. Neurobiol.* **54**, 7777–7788 (2017).
24. Wu, L. Y. et al. Roles of pannexin-1 channels in inflammatory response through the TLRs/NF- κ B signaling pathway following experimental subarachnoid hemorrhage in rats. *Front. Mol. Neurosci.* **10**, 175 (2017).
25. Wang, J. et al. Alpha-7 nicotinic receptor signaling pathway participates in the neurogenesis induced by ChAT-positive neurons in the subventricular zone. *Transl. Stroke Res.* <https://doi.org/10.1007/s12975-017-0541-7> (2017).
26. Stambanoni Bassi, M. et al. Amyloid- β homeostasis bridges inflammation, synaptic plasticity deficits and cognitive dysfunction in multiple sclerosis. *Front. Mol. Neurosci.* **10**, 390 (2017).
27. Neuhaus, W. et al. Multifaceted mechanisms of WY-14643 to stabilize the blood–brain barrier in a model of traumatic brain injury. *Front. Mol. Neurosci.* **10**, 149 (2017).
28. Chen, J. et al. Therapeutic benefit of intravenous administration of bone marrow stromal cells after cerebral ischemia in rats. *Stroke* **32**, 1005–1011 (2001).
29. Gao, Y. et al. Tetrahydrocurcumin reduces oxidative stress-induced apoptosis via the mitochondrial apoptotic pathway by modulating autophagy in rats after traumatic brain injury. *Am. J. Transl. Res.* **9**, 887–899 (2017).
30. Silvestre, J. S. et al. [Lactadherin promotes VEGF-dependent neovascularization]. *Med. Sci.* **21**, 683–685 (2005).
31. Boddaert, J. et al. Evidence of a role for lactadherin in Alzheimer's disease. *Am. J. Pathol.* **170**, 921–929 (2007).
32. Uchiyama, A. et al. Protective effect of MFG-E8 after cutaneous ischemia-reperfusion injury. *J. Invest. Dermatol.* **135**, 1157–1165 (2015).
33. Xiong, Y., Mahmood, A. & Chopp, M. Animal models of traumatic brain injury. *Nat. Rev. Neurosci.* **14**, 128–142 (2013).
34. Xu, J. et al. Luteolin provides neuroprotection in models of traumatic brain injury via the Nrf2-ARE pathway. *Free Radic. Biol. Med.* **71**, 186–195 (2014).
35. Zhou, C. et al. Decreased progranulin levels in patients and rats with subarachnoid hemorrhage: a potential role in inhibiting inflammation by suppressing neutrophil recruitment. *J. Neuroinflamm.* **12**, 200 (2015).
36. Aziz, M. M. et al. MFG-E8 attenuates intestinal inflammation in murine experimental colitis by modulating osteopontin-dependent alphavbeta3 integrin signaling. *J. Immunol.* **182**, 7222–7232 (2009).
37. Gao, Y. et al. Tetrahydrocurcumin provides neuroprotection in rats after traumatic brain injury: autophagy and the PI3K/AKT pathways as a potential mechanism. *J. Surg. Res.* **206**, 67–76 (2016).
38. Zhang, L., Ding, K., Wang, H., Wu, Y. & Xu, J. Traumatic brain injury-induced neuronal apoptosis is reduced through modulation of PI3K and autophagy pathways in mouse by FTY720. *Cell. Mol. Neurobiol.* **36**, 131–142 (2016).
39. Wang, Y. et al. sAAV9-VEGF prolongs the survival of transgenic ALS mice by promoting activation of M2 microglia and the PI3K/Akt pathway. *Brain Res.* **1648**, 1–10 (2016).
40. Zhao, Y. et al. Neuroprotective effect of fasudil on inflammation through PI3K/Akt and Wnt/beta-catenin dependent pathways in a mice model of Parkinson's disease. *Int. J. Clin. Exp. Pathol.* **8**, 2354–2364 (2015).
41. Cox-Limpens, K. E., Gavilanes, A. W., Zimmermann, L. J. & Vles, J. S. Endogenous brain protection: what the cerebral transcriptome teaches us. *Brain Res.* **1564**, 85–100 (2014).
42. Walker, C. L., Liu, N. K. & Xu, X. M. PTEN/PI3K and MAPK signaling in protection and pathology following CNS injuries. *Front. Biol.* **8**, <https://doi.org/10.1007/s11515-013-1255-1> (2013).